ABCM Symposium Series in Mechatronics - Vol. 1 - pp.254-263
Copyright © 2004 by ABCM

Evaluation of the robustness of H_∞ controllers applied to a flexible beam

Eurípedes Guilherme de Oliveira Nóbrega
Departamento de Mecânica Computacional
Faculdade de Engenharia Mecânica
Universidade Estadual de Campinas
egon@fem.unicamp.br

José Alberto de Araújo
Departamento de Engenharia Mecânica
Centro de Tecnologia
Universidade Federal do Rio Grande do Norte
Josalb@uol.com.br

Sérgio Issamu Matsumoto
Departamento de Mecânica Computacional
Faculdade de Engenharia Mecânica
Universidade Estadual de Campinas
sergio@fem.unicamp.br

Abstract: Active control of mechanical structure vibrations is a challenging problem imposed by the trend to adopt lighter and more flexible solutions for the engineering systems of today. Several difficulties make this application a hard one for the controller design. Any mechanical structure is continuous and presents infinite vibration modes. Using modal analysis, the respective mathematical modeling is in general represented as an infinite summation of modes, but truncated at a maximal frequency, accepted as the frequency range of interest. Such models are validated through experimental measurements, using an identification method which presents in general good approximation for the natural frequencies, but poor resolution for the damping factors and for the identification of zeros of the transfer matrix. These uncertainties are reflected at the position of the closed-loop poles, provoking the known phenomenon of spillover and often instability. On the other hand, it is common that the controllers are noncollocated and nonminimum phase, imposing limits to the performance of the systems. As a consequence of all these factors, considering the mechanical structures as uncertain systems is fundamental, demanding robust methods for the synthesis of the controllers. Studying the uncertainties to design weight filters in order to shape the frequency response of the controllers is one simple and common method. But it is necessary a tedious adjustment of the filters, which must be maintained as simple as possible, because their orders add to the final order of the controller. In this sense, each controller has to be particularly designed, and its success depends basically on the designer experience to correctly perceive all the trends in the behavior of the closed-loop systems. Exploring these facts, several H_∞ controllers were designed and experimentally tested, applied to a free-free flexible beam. Piezoelectric ceramics were used as control and disturbance actuators and a micro-accelerometer used to measure the vibration. The controller and filter designs are detailed and its characteristics and results are discussed and related to the structural and parametric uncertainties.

Keywords: *Flexible structure control, H_∞ control, robust control, active vibration control*

1. Introduction

Active control of flexible mechanical structures has been studied for some decades now, but it is still a very challenging problem with a rapid growing number of applications. Space structures are clearly very light and flexible and exposed to disturbing vibrations, demanding active control methods. But there is a general trend to design systems using lighter structures and many of them may benefit from these methods. This has been motivating the researchers worldwide, however conducting to some common pitfalls, whose solutions are not yet completely studied. The problems with these methods are in general related to the robustness of the controllers, and may be revealed even in the very simple structures. Spillover is the tendency for the plants to become unstable, based on the excitation of the out-of-bandwidth natural frequencies, named after the early work of Balas (1978). Enforcing the control signal to be void of the unwanted frequencies is the obvious solution, and the actual method of choice is to use an weight function with the appropriate spectrum to shape the desired frequency behavior (Fujimoto, 1995) (Kajiwara and Nagamatsu, 1995) (Gawronski and Lim, 1998). But also the in-bandwidth natural frequencies may cause trouble. The problem begins at the identification phase, where the zeros of the plant transfer function may not be well estimated. The dynamics of the mechanical structures are described by a particular partial differential equation, whose solution consists of an infinite number of terms. Considering modal analysis, the model is written as an infinite summation of vibration modes, corresponding to each natural frequency. To design a controller, a frequency range is specified according to the expected operating conditions of the plant. As a consequence, the model is truncated to include only a finite number of modes, which implies in the poor estimation of the open-loop zeros. Considering that these zeros impact in the closed-loop poles position, the final result is an uncertainty in the performance of the system, conducting eventually to instability. To overcome the zeros poor estimation, two methods are well known (Clark, 1997): including a zero frequency term in the truncated model, proportional to the sum of the effects of the omitted modes; or including an additional mode with resonant frequency much higher then the frequency range of interest, with an equivalent compliance of the omitted modes. The zero frequency term is equivalent to include a feedthrough matrix in a state-space model, implying that the transfer function now presents the same number of zeros and poles. A method to

optimize this term value, based on the H_2 norm of the error between the truncated and the infinite-dimensional model, is presented by Moheimani (2000). Experimentally, system identification frequency domain methods compute an upper frequency residual term based on least-square estimation, and also a lower frequency residual term, considering that the frequency range of interest may be an interval, ignoring lower and upper modes. But time domain identification methods are not capable of taking into account the residual terms, and these methods are commonly used to design a controller, particularly the eigensystem realization algorithm (ERA) (Juang, 1994), because they estimate the state-space matrices directly from the Markov parameters. Adopting this identification method, the zeros poor estimation are inevitable, and the consequent uncertainty is treated here.

A free-free flexible aluminum beam with piezoelectric actuators and a micro-accelerometer sensor was experimentally identified using the ERA method, and the correspondent models used to implement several different H_∞ controllers, aiming to study how to avoid the undesired effects of the spillover and of the uncertainties caused by the open-loop zeros, the parametric errors and the neglected out-of-bandwidth dynamics. To achieve a good performance of the controller, given an uncertain plant model, the main tool available to the designer is to shape adequately the weight filters. The active vibration control H_∞ problem is described in Section II and the beam model and experimental testbed is presented in the Section 3. The several weighting functions and its results are presented in Section 4, and the unstable behavior studied in the Section 5. Conclusion remarks are presented in Section 6.

2. H_∞ vibration control

The purpose of active vibration control is to design a controller to attenuate the vibration of the natural frequencies to acceptable levels, however assuring the closed-loop stability in the first place. Based on the reduced order model of the plant, an important objective is to avoid the influence of the upper residual frequencies in the system performance. As mentioned in the introduction of this paper, this means not to excite out-of-bandwidth natural frequencies, but also to guarantee that the in-bandwidth frequencies poles remain in the left complex half-plane. These two objectives are here considered separately.

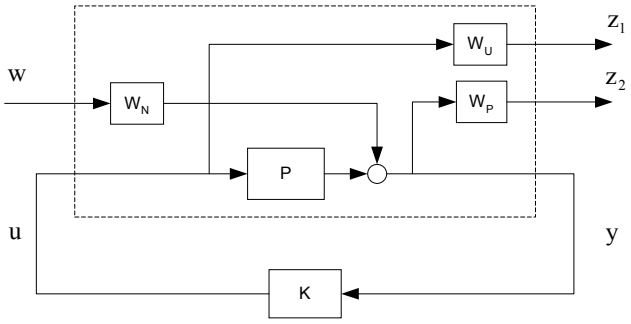

Figure 1. Block diagram of the H_∞ design scheme

Referring to Fig. (1), the control signal *u(t)* is weighted through the filter $W_u(s)$, in order to avoid the spillover, and the filter $W_p(s)$ is used to weight the measured output of the plant *y(t)* to achieve the vibration level reduction. It is been considered a disturbance input signal *w(t)* filtered at the input by $W_n(s)$ and two performance signals $z_1(t)$ and $z_2(t)$ respectively the outputs of the two output weighting filters. The plant nominal transfer function is *P(s)* and the *true plant model* is $P_t(s)$. The controller, assumed to satisfy the prescribed conditions, has the transfer function *K(s)*.

An input multiplicative uncertainty $\Delta(s)$ is assumed such that

$$P_t(s) = P(s)\big(I + \Delta(s)\big)$$

Admitting $\|\Delta(j\omega\| \le 1$, the small-gain theorem implies that

$$\left\|\Delta(j\omega)T_{z_1 w}(j\omega)\right\|_\infty < 1,$$

where $T_{z1w}(s)$ is the transfer function between the disturbance input and the performance signal $z_1(t)$. Designing the filter $W_u(s)$ such that $\left|W_u(j\omega)\right| > \left|\Delta(j\omega)\right|, \forall\omega$, the robust stability condition becomes

$$\left\|W_u(j\omega)T_{uw}(j\omega)\right\|_\infty < 1,$$

where $T_{uw}(s)$ is the transfer function between the disturbance input and the control signal. This takes care of the first objective, avoiding the spillover, as long as the filter $W_u(s)$ presents a realistic compatible frequency distribution about the uncertainties. In order to achieve vibration attenuation, the measured plant output must satisfy

$$\left\| W_p(j\omega) T_{yw}(j\omega) \right\|_\infty < 1 ,$$

where $T_{yw}(s)$ is the transfer function between the disturbance input and the measured output. These two inequalities may be stacked together, forming the mixed sensitivity problem described by

$$\left\| \begin{matrix} W_u(j\omega) T_{uw}(j\omega) \\ W_p(j\omega) T_{yw}(j\omega) \end{matrix} \right\|_\infty < 1 ,$$

which may be solved using the standard H_∞ design approach (Skogestad and Postlethwaite, 1996). This is an usual method to solve the active vibration control, but notice that the parametric uncertainty due to the estimation errors has not been taking into account. In the following sections, some results are presented showing the consequences of this omission.

3. Plant model and identification

3.1 Nominal plant model

A flexible structure with a limited number of sensors and actuators may be mathematically represented by an infinite summation of modes such as

$$P_t^{kj}(s) = \frac{Y^k(s)}{U^j(s)} = \sum_{i=1}^{\infty} \frac{F_i^{kj}}{s^2 + 2\zeta\omega_i s + \omega_i^2} ,$$

where each ω_i is a natural frequency, ζ_i is the respective modal damping, the parameters F_i^{kj} are dependent of the input position of actuator j and output position of sensor k, $Y^k(s)$ is the Laplace transform of the measured output at sensor k and $U^j(s)$ is the Laplace transform of the applied force to actuator j. This infinite dimensional transfer function is in general truncated at a modal index N, corresponding to the number of degree of freedom (DOF) considered, reflecting the knowledge of the operational conditions of the system. Considering the N modes to be included in the bandwidth of the controller, and dropping the input/output indexes for the sake of simplicity, the structure may be represented as

$$\begin{aligned} P(s) &= \sum_{i=1}^{N} \frac{F_i}{s^2 + 2\zeta\omega_i s + \omega_i^2} \\ P_R(s) &= \sum_{i=N+1}^{\infty} \frac{F_i}{s^2 + 2\zeta\omega_i s + \omega_i^2} , \\ P_t(s) &= P(s) + P_R(s) \end{aligned}$$

where, $P_R(s)$ refers to the residual modes. Each mode must satisfy the ordinary differential equation

$$\frac{d^2 y_i}{dt^2} + 2\zeta\omega_i \frac{dy_i}{dt} + \omega_i^2 y_i = b_{mi1} f_i + b_{mi2} d_i ,$$

where $y_i(t)$ is the respectively measured position, $b_{mi1} f_i$ is the actuator input and $b_{mi2} d_i$ is an actuator disturbance. Considering a state-space vector defined as $x^T = \begin{bmatrix} y & \dot{y} \end{bmatrix}$, the state-space model for N DOF may be written as

$$\begin{aligned} \dot{x} &= Ax + B_1 w + B_2 u \\ y &= Cx + D_{21} w \end{aligned}$$

where each matrix has the appropriate dimension and is defined according to

$$A = \begin{bmatrix} 0_N & I_N \\ -\Lambda & -\Xi \end{bmatrix} \quad B_1 = \begin{bmatrix} 0 \\ \Phi^T B_{m1} \end{bmatrix} \quad B_2 = \begin{bmatrix} 0 \\ \Phi^T B_{m2} \end{bmatrix},$$

where B_{m1} is the matrix formed with the elements b_{mi1} and B_{m2} is the matrix formed with the elements b_{mi2}, Φ is the modal matrix satisfying the normalization

$$\Phi^T M \Phi = I_N$$

where M is the mass matrix of the plant. The stiffness matrix Λ and the damping matrix Ξ is defined according to

$$\Lambda = diag(\omega_1^2, \omega_2^2, \ldots, \omega_N^2), \; \Xi = \Phi^T C \Phi$$

3.2 Testbed description

An aluminum beam with length of 1100 mm, height of 32 mm and width of 3 mm, hanging from the ceiling through nylon wires, was used to evaluate several designed controllers. The respective instrumentation comprises two piezoelectric actuators model QP10N and respective power amplifier model EL 1224 from Active Control Experts, a micro-accelerometer Kistler, model 8614 and signal conditioner model 5134, and Frequency Devices filters model 900C/9L8B. A dSPACE board model DS1003 with 16 bits analog-to-digital and 14 bits digital-to-analog converters and a Texas Instruments digital signal processor TMS320C40 was used to acquire data from the accelerometer and produce the disturbance and control input signals. The complete scheme representing the experiments is depicted in Fig. (2).

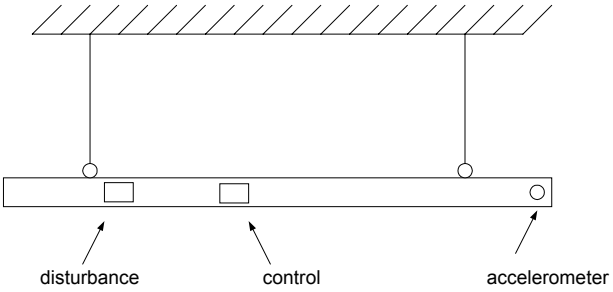

2a)

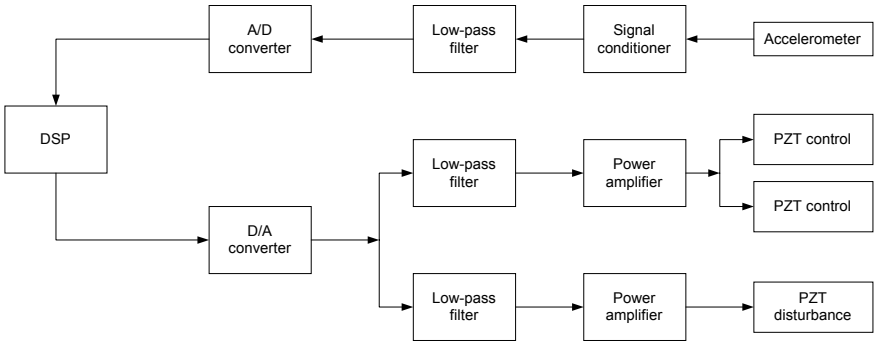

2b)

Figure 2. Free-free beam experimental scheme: a) actuators and sensors b) instrumentation

Table 1. Modes and frequencies of the aluminum beam

Mode	Frequency (Hz)
1	36.1
2	70.4
3	115.3
4	172.9
5	242.7

To identify the plant, a Schroeder signal, presenting a flat amplitude spectrum from 0 to 250 Hz, was applied to both inputs. There are two PZTs patches at the central position, a second one at the opposite side of the beam, not shown in Fig. (2), and another PZT patch at the left. The control input is considered the central pair of PZT patches and the disturbance input is the left patch. The output is the accelerometer signal, at the right tip of the beam. By virtue of

this scheme, the plant model presents two inputs and one output. Several frequency response functions were calculated and averaged generating the Markov parameter used in the eigensystem realization algorithm. Two models were determined. The first model includes three modes and is considered the uncertain plant model. The second model includes 5 modes, with two higher frequencies modes then the three modes of the plant model. All frequencies and modes are presented at Table (1), up to 250 Hz. The aluminum beam has other modes in the same band, but they are not being excited by the PZTs. The second model is used to test the controllers with frequencies beyond the bandwidth of interest, considered 125 Hz for these analyses.

The discrete state-space matrices for these two models, for a sample frequency of 1000 Hz, are

$$A = \begin{bmatrix} 0.6340 & -0.7705 & 0.0022 & 0.0144 & 0.0012 & 0.0006 \\ 0.7705 & 0.6312 & -0.0329 & -0.0186 & 0.0053 & 0.0010 \\ 0.0023 & 0.0328 & 0.1043 & 0.9842 & 0.0038 & 0.0008 \\ -0.0144 & -0.0186 & -0.9842 & 0.1175 & -0.0110 & -0.0022 \\ -0.0007 & -0.0022 & -0.0021 & 0.0030 & 0.8961 & 0.4331 \\ -0.0001 & 0.0007 & 0.0005 & -0.0009 & -0.4331 & 0.9012 \end{bmatrix}, \quad B = \begin{bmatrix} 0.1380 & -0.2142 \\ -0.0663 & 0.1228 \\ 0.1850 & -0.3340 \\ -0.0697 & 0.1057 \\ 0.0792 & 0.0947 \\ -0.0101 & -0.0200 \end{bmatrix}$$

$$C = \begin{bmatrix} 0.2550 & 0.1393 & 0.3822 & 0.1263 & -0.1213 & -0.0231 \end{bmatrix}, \quad D = \begin{bmatrix} 0 & 0 \end{bmatrix}$$

for the plant model and

$$A = \begin{bmatrix} 0.6338 & -0.7705 & -0.0009 & 0.0156 & -0.0003 & 0.0071 & 0.0006 & 0.0118 & 0.0009 & 0.0006 \\ 0.7703 & 0.6311 & -0.0359 & -0.0166 & -0.0165 & 0.0089 & 0.0012 & 0.0159 & 0.0047 & 0.0011 \\ -0.0012 & 0.0333 & 0.0711 & 0.9786 & -0.0061 & 0.1093 & 0.0031 & 0.0643 & 0.0001 & 0.0001 \\ -0.0149 & -0.0162 & -0.9690 & 0.0964 & 0.1359 & -0.1119 & -0.0047 & -0.0740 & -0.0096 & -0.0022 \\ 0.0027 & -0.0065 & 0.0243 & 0.0942 & -0.5685 & -0.8127 & -0.0017 & -0.0282 & 0.0038 & 0.0008 \\ 0.0125 & 0.0094 & 0.1603 & 0.0479 & 0.8052 & -0.5462 & 0.0035 & 0.0592 & 0.0131 & 0.0031 \\ -0.0003 & 0.0006 & -0.0013 & -0.0024 & -0.0010 & -0.0004 & -0.9971 & 0.0762 & -0.0002 & -0.0001 \\ 0.0126 & -0.0098 & 0.0653 & 0.0703 & 0.0408 & 0.0331 & -0.0748 & -0.9628 & 0.0258 & 0.0057 \\ -0.0010 & -0.0019 & -0.0056 & 0.0030 & -0.0048 & 0.0114 & 0.0016 & 0.0233 & 0.8961 & 0.4331 \\ -0.0001 & 0.0007 & 0.0011 & -0.0011 & 0.0008 & -0.0025 & -0.0004 & -0.0055 & -0.4331 & 0.9012 \end{bmatrix}, \quad B = \begin{bmatrix} 0.1367 & -0.2181 \\ -0.0668 & 0.1237 \\ 0.1448 & -0.3919 \\ -0.0688 & 0.0668 \\ 0.1035 & 0.1911 \\ 0.2186 & 0.1011 \\ 0.0082 & -0.0103 \\ 0.0840 & 0.3934 \\ 0.0727 & 0.0814 \\ -0.0104 & -0.0201 \end{bmatrix}$$

$$C = \begin{bmatrix} 0.2603 & 0.1419 & 0.4438 & 0.0946 & 0.2307 & -0.1807 & -0.0268 & -0.3902 & -0.1071 & -0.0237 \end{bmatrix}, \quad D = \begin{bmatrix} 0 & 0 \end{bmatrix}$$

for the second model. The respective Bode diagrams of these plants are presented in Fig. (3).

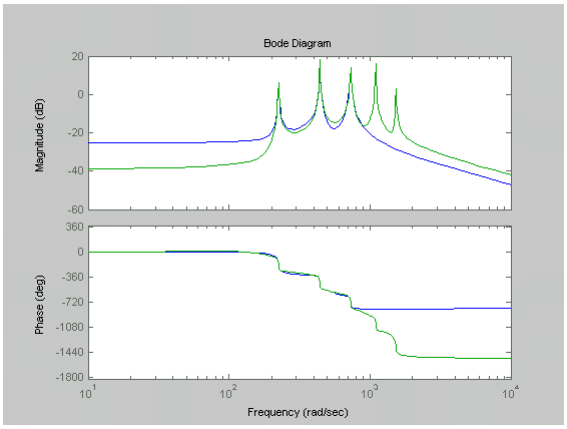

Figure 3. Bode diagrams of the nominal plant and extended plant models

4. Weighting filters

Several filters were designed and tested. The disturbance input filter is simply a gain $W_n = 0.08$. The control input filter W_u is designed according to the uncertainty of the plant model. In this case, the uncertainty beyond 125 Hz is 100 %. The resulting filter is a high-pass

$$W_u = \frac{0.0005\,s + 0.1}{0.00025\,s + 1},$$

whose Bode diagram is presented in Fig. (4).

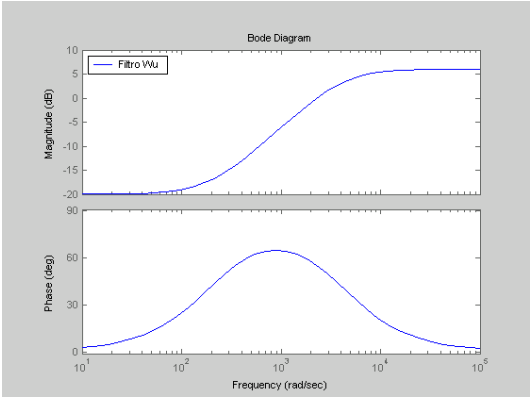

Figure 4. Bode diagram of the control input filter

The output filter W_p is a low-pass, which reflects the desired behavior of the controller. It must attenuate the low frequency band and let the high frequency band pass. Recall that the effect in the respective filtered signal correspond to the inverse filter. It is supposed that no high frequency will be excited by the control signal, because of the respective filter W_u. Considering that the order of the controller is the orders of the plant plus the order of the filters, unless a reduced order controller design is used, which is beyond the scope of this work, it is interesting to maintain the order of the filters as small as possible. For this reason, first order filters were adopted, even if second order filters could eventually get better results. One of the output filters tested (cnt07, see Table (2)), with adequate attenuation levels, is

$$W_p = \frac{2.1133\,s + 3170}{s + 1000},$$

whose Bode diagram is presented in Fig. (5).

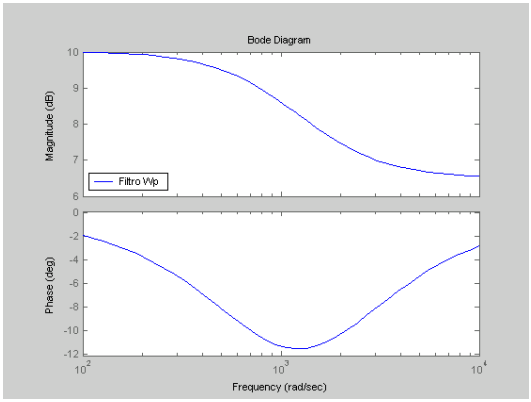

Figure 5. Bode diagram of a typical output filter

5. Experimental results

To conduct the tests several values for the poles, zeros and static gain of the filter W_p were adopted. Table (2) presents the respective values

Table 2. Different output filters tested

Cont.	G0 (dB)	Pole	Zero	Observations
cnt01	20	200	800	Stable
cnt02	20	200	1500	Stable
cnt03	20	500	1500	Not tested because of too low value of matrix element (2,25e-52)
cnt04	20	800	1500	Worked properly
cnt05	20	800	2000	Unstable
cnt06	20	1000	1500	Unstable
cnt07	10	1000	1500	Worked properly
cnt08	10	1000	2000	Stable
cnt09	10	800	1500	Not tested because of value (7e-295)

Nine controller design were tested, with two unstable closed-loop, two with numbers that were two small for the dSpace software to deal with, and five stable closed-loop. From the stable controllers, two were chosen to further analyses. For the controller cnt07 and controller cnt04, the tonal results for the three natural frequencies is presented in Fig. (6), and the results for the out-of-bandwidth two frequencies are presented in Fig. (7). The controller cnt07 results are on the left part of the figures.

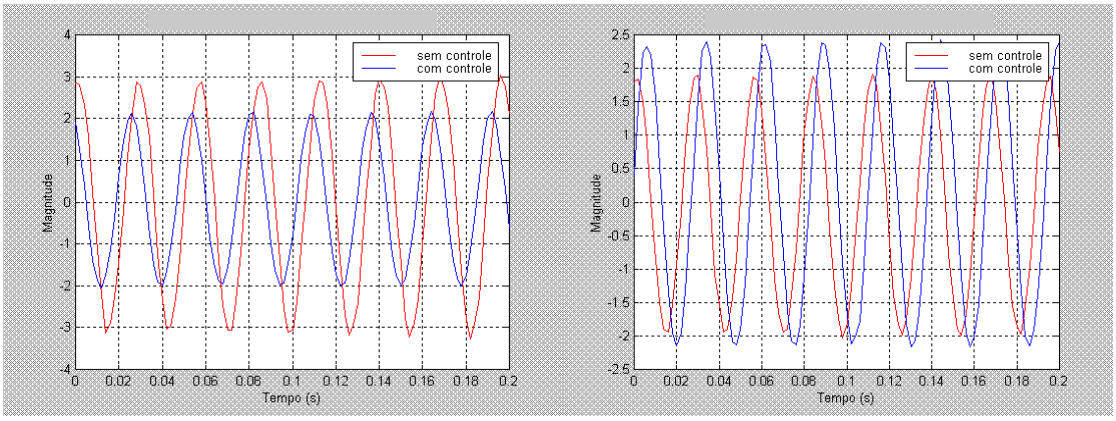

6a)

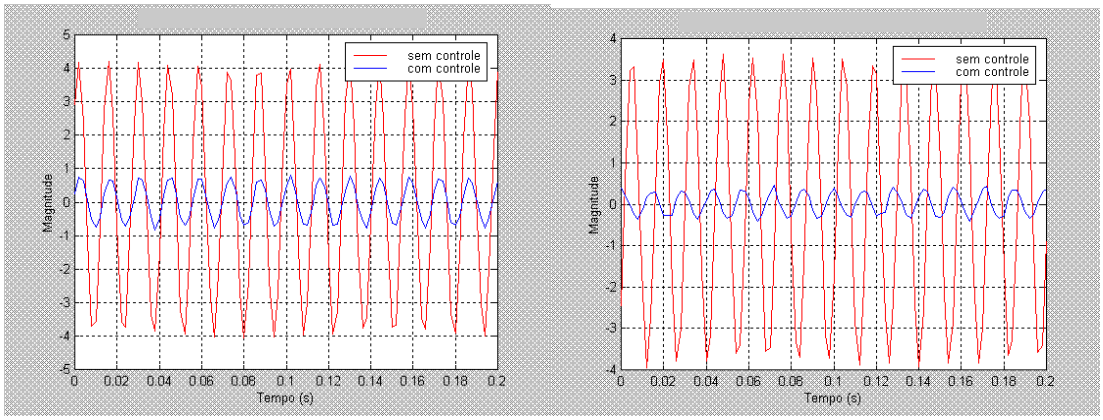

6b)

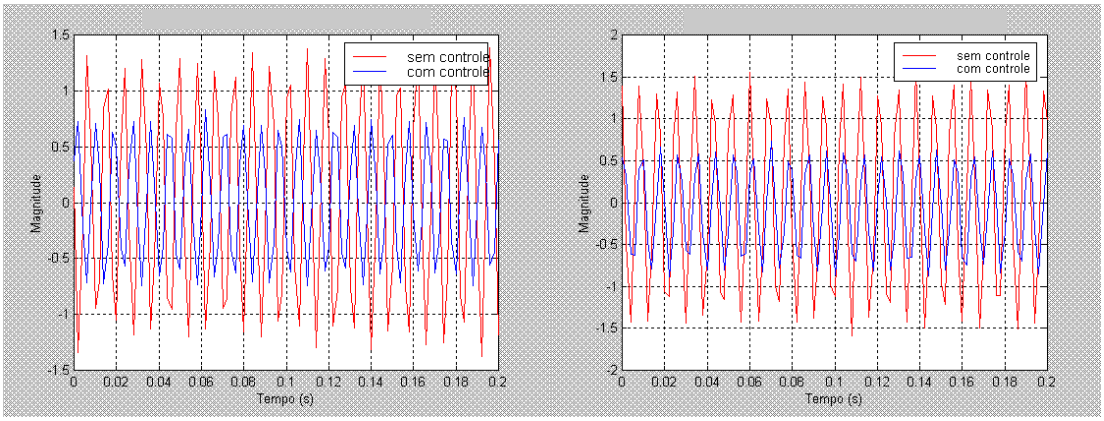

6c)

Figure 6. Tonal results for the in-bandwidth frequencies for controller 7. a) first natural frequency at 36.1 Hz b) second frequency at 70.4 Hz c) third frequency at 115.3 Hz. Results for controller cnt07 are on the left and for controller cnt04 are on the right

For the controller cnt07, an attenuation of approximately 6 dB for the first natural frequency, of 15.6 dB for the second and 5.4 dB for the third frequency is seen in Figs. (6a), (6b) and (6c), respectively. For the controller cnt04, an

attenuation of approximately 2 dB for the first natural frequency, of 20.8 dB for the second and 8 dB for the third frequency is seen in Figs. (6a), (6b) and (6c), respectively.

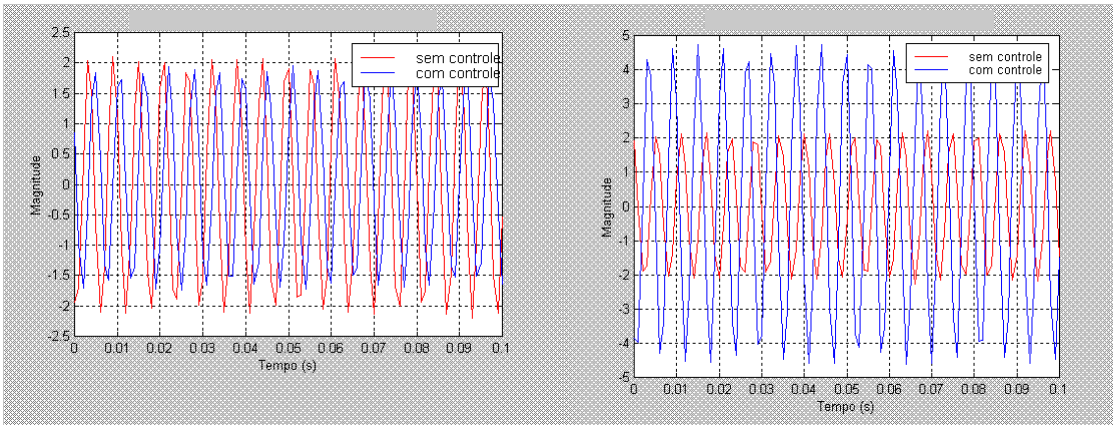

7a)

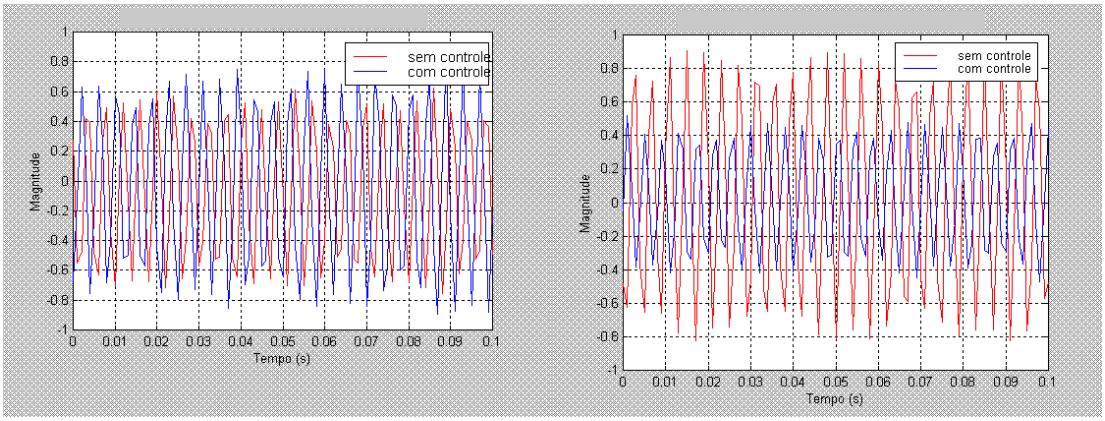

7b)

Figure 7. Tonal results for the out-of-bandwidth frequencies for controllers cnt07 (to the left) and cnt04 (to the right). a) fourth natural frequency at 172.9 Hz b) fifth natural frequency at 242.2 Hz

In Figure (7) the behavior of the closed-loop system for the two out-of-bandwidth natural frequencies is presented. It may be seen from Fig. (7a) for the controller cnt07 that a small attenuation is present for the fourth natural frequency of approximately 2 dB, but for the fifth frequency a small amplification of the same order is visible. For the controller cnt04 a bigger attenuation of 6.5 dB in clearly visible for the forth frequency and also 6 dB of attenuation for the fifth frequency, which is the opposite of controller cnt07 that amplified this frequency.

To understand the apparently distinct behavior for closed-loop systems not so different, a root locus was plotted for both controllers, where a proportional gain multiplying the controller output is varying. The result for controller cnt07 is shown in Fig. (8), and for controller cnt04 is in Fig. (9).

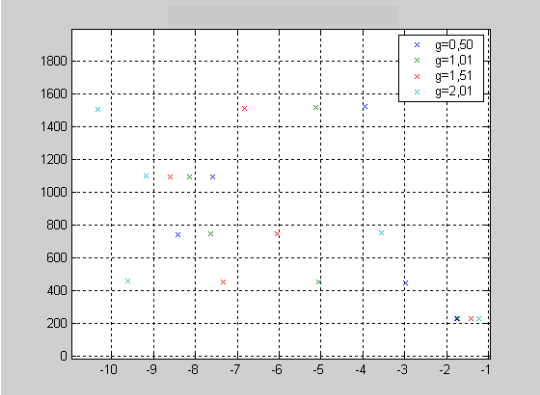

Figure 8. Root locus using the controller cnt 07 with varying gain

In Figure (8) the five poles are represented in the upper half left complex plane, for four values of the gain. It may be seen that each pole has its own behavior when the gain is increased. The pole of the first natural frequency varies only a little, but it approximates the imaginary axis as the gain increases. The pole of the second natural frequency present a bigger variation, but in the opposite direction, meaning that it will never cause an instability. The third pole also varies significantly, and in the direction of the instability. The fourth pole presents a small variation, not so small as the first one, and in the good direction, away from the imaginary axis. The fifth pole is varying also in the good direction and with big steps. The obvious conclusion here is that the out-of-bandwidth poles are not impacting on the stability of the closed-loop system, at least for this controller, and that a compromise could be achieved between the attenuation levels of the second and the third natural frequencies. Recall that the imaginary part of the pole is much bigger than the real part, implicating in very small damping factors, and by this reason the relative size of the real part comparing for the same varying pole is approximately the relative variation of the damping factor.

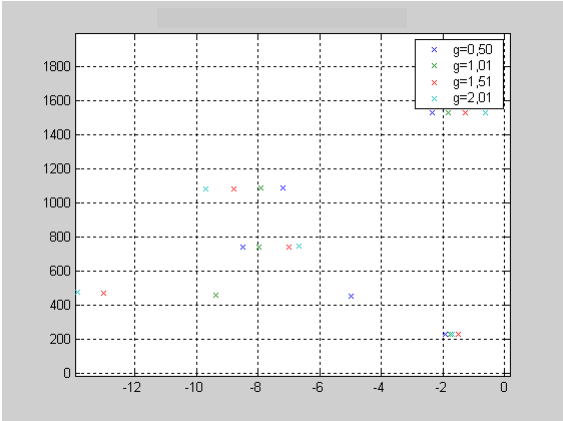

Figure 9. Root locus using the controller cnt04 with varying gain

Regarding the root locus of Fig. (9), the first frequency remains close to each other in a similar way to the other controller; the second frequency is getting away from the imaginary axis, also in a similar fashion to cnt07; the third frequency is approximating to the imaginary axis, but more slowly then the previous case; the forth frequency is getting far from the imaginary axis in a similar behavior to the cnt07 and the fifth frequency is getting close the imaginary axis, in an opposite direction comparing to controller cnt07, aggravated by small absolute values. This means that this frequency now may pose a problem to the stability of the system.

The reason why some frequencies goes to one side and others the opposite side are related to the zeros positions of the system. Because this is a noncolocated plant, the system is nonminimum phase, with the right plane zeros attracting some poles. And because the zeros of the plant have a great degree of uncertainty the actual behavior of the experimental system may be very different from the simulated results obtained through controller design. This is consistent with the fact that all controllers at Table (2) presented good performance when designed, but some of then resulted unstable when implemented. To be sure that the expected performance is achieved experimentally the correct position of the zeros must be evaluated more closely, and all zeros of the plant for the measured position must be represented in the identified transfer function. Besides, considering the small damping factors of these systems and consequent proximity of the imaginary axis of the poles, parametric uncertainty must be included in the plant model to prevent error in the closed-loop pole positions.

6. Conclusions

To design an active controller to attenuate the vibrations of mechanical structures an uncertainty model from the out-of-bandwidth frequency range must be included. The main tool available to the designer to improve the robustness of the closed-loop system is to consider all frequency distribution knowledge about the plant and embed it into the design of the weight filters. But this may not be enough to ensure performance and even stability, if the zeros of the plant are not adequately estimated. Also, the parametric uncertainty concerning these zeros are important to be included in the uncertain model of the plant, which must include the uncertainty from the poles also.

7. Referências

Balas, M. J., Feedback Control of Flexible Systems, IEEE Transactions, AC-23, No. 4, 1978, pp. 673-679

Clark, R. L., Accounting for Out-of-Bandwidth Modes in the Assumed Mode3s Approach: Implications on Colocated Output Feedback Control, Transactions of the ASME, V. 119, September 1997, pp. 390-395

Fujimoto, T., Vibration Control of a Cantilever Beam Using a H_∞ Controller for Noncolocated Systems, IEEE International Conference on Intelligent Systems for the 21st Century, V. 1 , 1995, pp. 557-562

Gawronski, W. and Lim, K. B., Frequency Weighting for the H_∞ and H_2 Control Design of Flexible Structures, J. Guidance, V. 21, No. 4, pp. 664-666

Juang, J-N, Applied System Identification, NASA Prentice-Hall, 1994

Kajiwara, I. & Nagamatsu, A., H_∞ Control System by Modal Analysis for Suppression of Structural Vibration" Proceedings of the 15th ASME Conf. Modal Analysis, Modelling, Diagnostic and Control, Analytical and Experimental, 1995, pp. 591-597.

Moheimani, S. O. R., Minimizing the Effect of Out of Bandwidth Modes in Truncated Structure Models, Journal of Dynamic Systems, Measurement and Control, V. 122, March 2000, pp. 237-239

Skogestad, S. & Postlethwaite, I., Multivariable Feedback Control Analysis and Design, John Wiley & Sons, 1996

8. Copyright Notice